energies

MDPI

Article

Experimental Validation for Moving Particle Detection Using Acoustic Emission Method

Sung-Wook Kim [1], Nam-Hoon Kim [2], Dong-Eon Kim [2], Tae-Han Kim [3], Dong-Hoon Jeong [3], Young-Hwan Chung [3] and Gyung-Suk Kil [2,*]

[1] Division of Smart Electrical & Electronic Engineering, Silla University, Busan 46958, Korea; number1@silla.ac.kr
[2] Department of Electrical and Electronics Engineering, Korea Maritime and Ocean University, Busan 49112, Korea; dom0404@kmou.ac.kr (N.-H.K.); jklfds1003@g.kmou.ac.kr (D.-E.K.)
[3] High Voltage Insulation Research Team, Power & Industrial Systems R&D Center, Hyosung Corporation, Changwon 51529, Korea; thkim2008@hyosung.com (T.-H.K.); jdh0330@hyosung.com (D.-H.J.); gozip@hyosung.com (Y.-H.C.)
* Correspondence: kilgs@kmou.ac.kr; Tel.: +82-51-410-4893

Abstract: Gas-insulated switchgears (GISs) are important pieces of power equipment used to improve the reliability of power facilities. As the number of GISs increases, more insulation failures occur every year. The most common cause of insulation failure is particles and foreign bodies producing a partial discharge (PD), which causes deterioration of the insulation materials and results in insulation breakdown. However, it is not easy to detect them by conventional PD and ultra-high frequency (UHF) PD measurements because it is difficult to apply the conventional method to the GISs in service, and the UHF method is not always applicable to GISs. Therefore, an appropriate method to detect particles and foreign bodies in GISs is needed. In this study, experimental validation was performed to detect particles moving in GISs using the acoustic emission (AE) method. Acoustic wave signals were produced by the particles moving on the surface of a flat plate when applying voltage. An AE sensor with a frequency range of 50 to 400 kHz was used, and a decoupler and low-noise amplifier were designed to detect the acoustic wave signals with high sensitivity. Twelve types of particles were used, and one was selected to confirm the detectable minimum output voltage. In an actual factory test, the output voltage of the acoustic wave signals was analyzed while considering the applied voltage and signal attenuation. Consequently, it was confirmed that the AE measuring system proposed in this paper could detect particles moving inside GISs.

Keywords: gas insulated switchgears; moving particles; acoustic emission method

Citation: Kim, S.-W.; Kim, N.-H.; Kim, D.-E.; Kim, T.-H.; Jeong, D.-H.; Chung, Y.-H.; Kil, G.-S. Experimental Validation for Moving Particle Detection Using Acoustic Emission Method. *Energies* **2021**, *14*, 8516. https://doi.org/10.3390/en14248516

Academic Editor: Wojciech Sikorski

Received: 6 November 2021
Accepted: 15 December 2021
Published: 17 December 2021

1. Introduction

Gas-insulated switchgears (GISs) have been used to protect electrical power systems in substations since the 1960s and are among the most valuable assets to provide reliable electric power. A GIS is composed of a gas circuit breaker, a voltage transformer, a current transformer, among other components, and is filled with SF6 gas, which has excellent insulation performance and arc-quenching capability. However, as the number of installed GISs has increased rapidly to improve the capacity and reliability of power facilities, insulation failure of GISs occurs every year. In an investigation by the CIGRE working group (A3.06), the major failure frequency (MaF) rate for GISs was 0.37 per 100 CB-bay-years. This shows that the MaF was 3 times higher than the target failure rate recommended by IEC 60071-2, which is 0.1 MaF per 100 CB-bay-years for GIS insulation coordination [1,2].

A total of 30% of dielectric GIS failures are related to design deficiencies, and other failures are related to quality assurance problems. Among them, the most frequent cause of GIS failure is particles, which account for 20% of the total, as shown in Figure 1 [3,4]. Particles are the most common defects occurring on site because they can enter the GIS

compartments despite the precautions taken during the GIS assembly process or can be produced due to mechanical vibration and incomplete impact during close–open operations, and it is hard for on-site engineers to detect them by visual inspection without any measuring equipment. Partial discharge (PD) occurs due to these particles and causes progressive deterioration of the insulation materials, and finally results in GIS failure. For this reason, many studies on the detection of particles have been performed with the electrical measurement for PD signals and mechanical vibration measurement for acoustic emission (AE) signals [5–11].

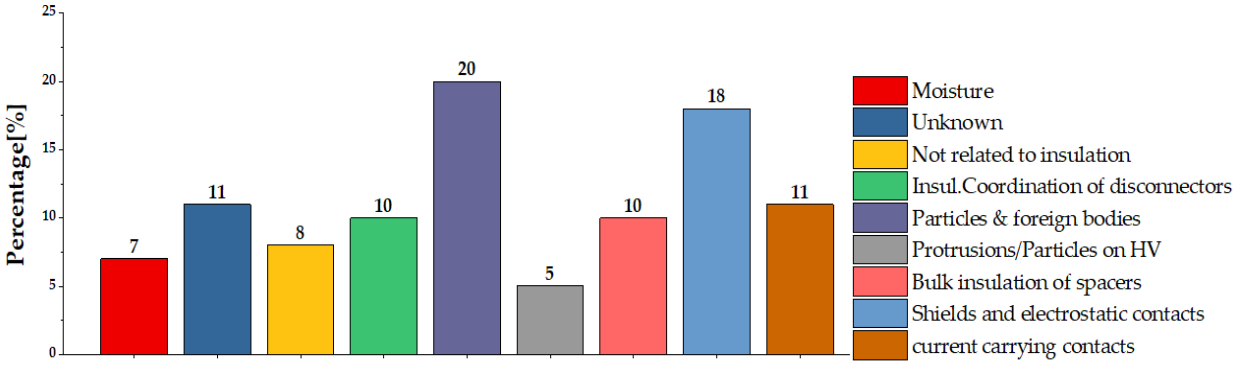

Figure 1. Mean distribution of dielectric failures in service. (Data sourced from: CIGRE).

In electrical measurement, the PD value by particles is a 5pC apparent charge for the conventional PD method specified in IEC 60270 [5] or an equivalent value for the ultra-high frequency (UHF) and acoustic emission (AE) methods in IEC 62478 [12]. The conventional method is accepted as the standard for PD measurement because the magnitude of the voltage signal measured by the coupling devices and measuring instruments can be calibrated in pC. The UHF method has a high sensitivity when internal PD sensors are used and good performance to identify the different types of PDs [13–19]. However, the conventional method is very difficult to apply to the GISs in service at high voltage levels. The UHF method is not always applicable to all types of GISs, and there are many cases in the field where internal sensors are not installed in the GISs [20].

The particles can move along the enclosure or lift off and jump toward the HV conductor, depending on their length and materials. Eventually, breakdown will occur. In a mechanical vibration measurement, the mechanical vibration by the particles moving and jumping in the GIS produces a strong acoustic wave signal that is easily detectable by the AE method. In addition, the AE method can be less sensitive to electrical noise interference and can locate moving particles because it is easy to carry and install AE equipment on GIS compartments. However, it is not easy to measure acoustic wave signals due to their complex characteristics, such as attenuation and reflection, so it is difficult to identify the physical conditions of the moving particles, such as their material, length, and diameter, which significantly influences GIS insulation [21–24]. Table 1 shows a comparison of the conventional and unconventional methods for PD measurement of GISs.

This paper describes the experimental validation of moving particle detection using the AE method to prevent failure of in-service GISs. The acoustic wave signals were produced by the particles moving on the surface of a flat plate when applying voltage. Twelve particles of different materials and diameters were fabricated considering the length condition of detectable and critical defects. An AE sensor with a frequency range of 50 to 400 kHz was used, and a decoupler and low-noise amplifier were designed to detect acoustic wave signals with high sensitivity. The particles that produced the lowest magnitude of acoustic wave signals were selected and applied to an actual factory test. In the actual factory test, the output voltage of the acoustic wave signal could detect the part s was analyzed while considering the applied voltage and signal attenuation. Consequently, it was confirmed that the AE measuring system proposed in this paper icles moving inside the GIS.

Table 1. Comparison of conventional and unconventional methods.

PD Methods	Conventional Method (IEC 60270)	Unconventional Methods	
		UHF	AE
Strengths	▪ Calibrated in pC ▪ High Sensitivity	▪ High Sensitivity (Internal sensor) ▪ Possible to locate PD	▪ Easy to carry and install ▪ Always applicable ▪ Possible to locate PD
Weakness	▪ Difficult to apply to GISs in service ▪ Not possible to locate PD	▪ Not Calibrated in pC ▪ Not always applicable	▪ Not Calibrated in pC ▪ Sensitive to external conditions

2. Experimental System

To detect mobile particles in the GIS easily, an AE sensor (R15I-AST, Physical Acoustics, Princeton JCT, Clarksville, NJ, USA) with a resonant frequency in the range of 150 kHz was used to detect the acoustic wave signals. The AE sensor is comparatively cheap and easy to carry, so it has good applicability when gaining access to a GIS gas compartment. However, the sensitivity of the sensor is highly dependent on the defect type and location, and separate cables for the power and signal lines are not provided. In this paper, therefore, a decoupler was designed to separate the acoustic signal from the power source, and a low-noise amplifier with wideband characteristics was designed to acquire 40 gains.

Figure 2 shows the designed decoupler with its circuit and frequency response characteristics. From the LC filter with C2 and L1, the high-frequency component of the DC source is not passed to the AE sensor, and only DC voltage is supplied to the sensor. The acoustic wave signal detected by the AE sensor is passed through C4 to the low-noise amplifier and is not passed to the DC source by the LC filter with C3 and L1. The frequency response characteristics of the decoupler designed in this paper shows that acoustic wave signals of 10 kHz or higher that are passed to the DC source from the AE sensor are attenuated to 150 dB and passed to the amplifier input as R2 without any attenuation.

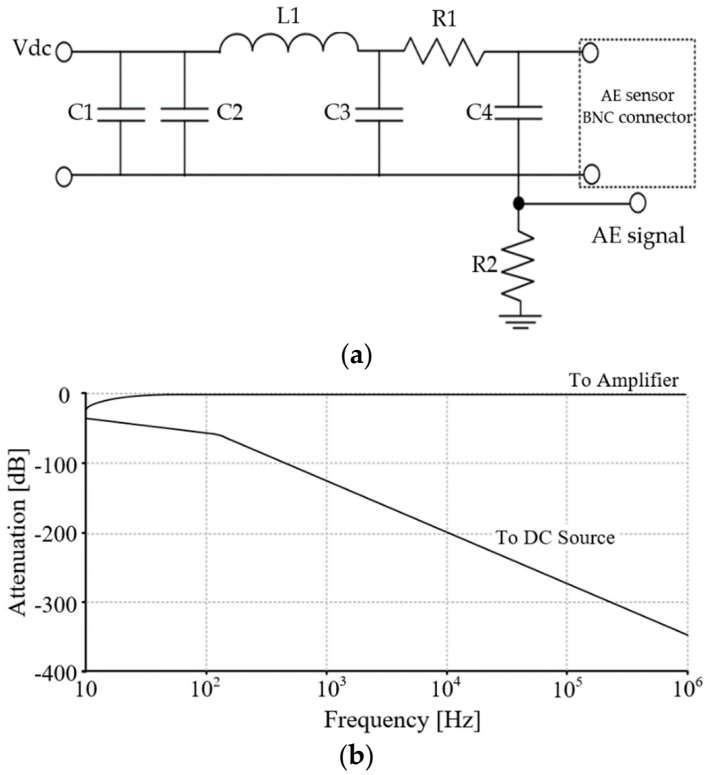

Figure 2. Decoupler: (**a**) circuit diagram, (**b**) frequency response graph.

Figure 3 shows the designed low-noise amplifier with the circuit and the frequency response characteristics. A low-noise operational amplifier with a DC gain bandwidth to 140 MHz was used to have wideband characteristics with a gain of 40 dB. The frequency response of the low-noise amplifier was analyzed by the ratio of the output voltage to the sine-wave input voltage from 11 kHz to 4 MHz using a signal generator. It has a low cut-off frequency of 11 kHz and a high cut-off frequency of 4 MHz at −3 dB [25,26].

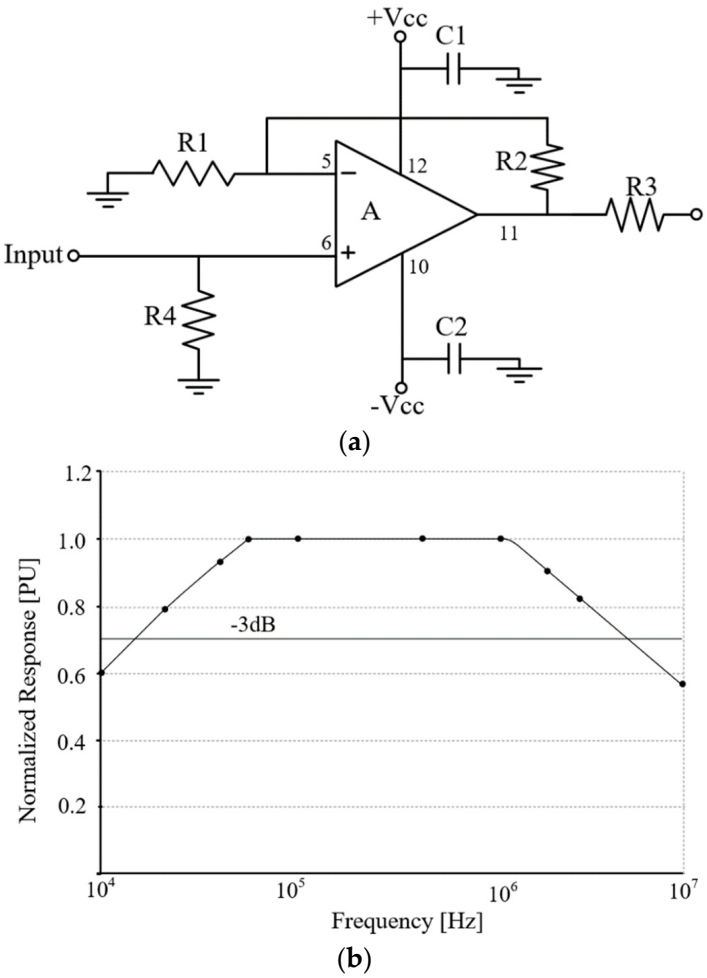

Figure 3. Low-noise amplifier: (**a**) circuit diagram, (**b**) frequency response graph.

To measure the acoustic wave signals produced by the vibration of the moving particles, an experimental setup was used as shown in Figure 4. Each particle was placed inside an acrylic chamber and the acoustic wave signal was detected by the AE measuring system, including an AE sensor, a decoupler, and a low-noise amplifier. The distance between the flat steel plates was 18 mm, and a noise cutting transformer (PTR220-03S, Primesolution Corporation, Gunpo, Gyeonggi-do, Korea) was used to minimize the external electrical noise of the power frequency. The 12 types of fabricated particles are shown in Table 2. The particles were aluminum, copper, and iron materials with diameters of 0.25 and 0.5 mm, which are the most common materials and diameters that occur on-site during the GIS assembly or operating process. The critical and detectable lengths of the moving particles were 3 to 5 mm, as specified by the CIGRE report [3]. The volume was calculated by using the diameter and the length. Depending on the moving particle, output voltage was recorded by OSC (MSO 5204, Tectronix, Beaverton, OR, USA) with a frequency range of 1 Hz to 2 GHz with a sampling rate of 10 GS/s when the particle was jumping and dropping on the surface of the flat steel plate due to the applied voltage.

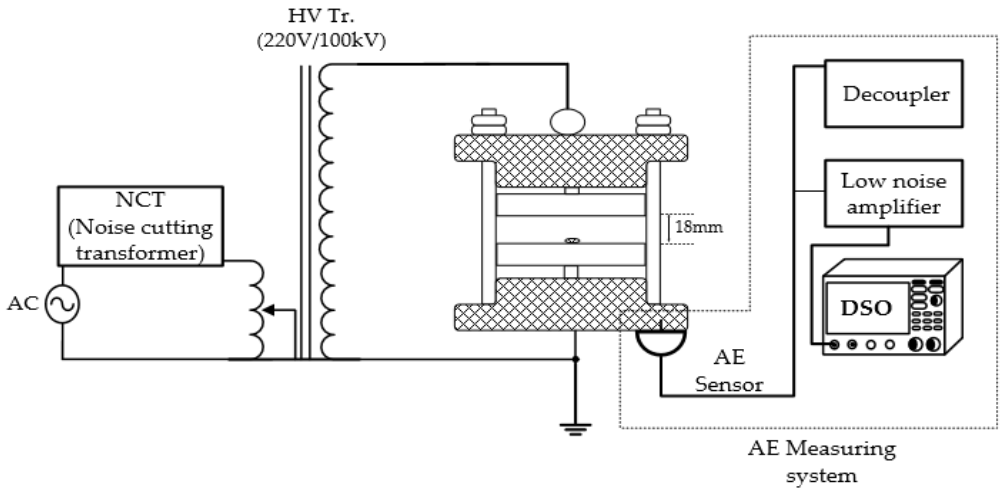

Figure 4. Experimental setup.

Table 2. Types of moving particles.

Materials	Diameter (mm)	Length (mm)	Volume (mm^3)
Aluminum	0.25	3	0.2
		5	0.3
	0.5	3	0.6
		5	1
Copper	0.25	3	0.2
		5	0.3
	0.5	3	0.6
		5	1
Iron	0.25	3	0.2
		5	0.3
	0.5	3	0.6
		5	1

3. Measurement and Analysis

The acoustic wave signals produced by the moving particles were measured. The movement of each particle was visually checked as the voltage to the acrylic chamber was increased in 1 kV increments. The acoustic wave signals produced when the particles jumped and dropped on the surface of the flat steel plate were measured by the AE measuring system. Figure 5 shows examples of the moving particles in the acrylic chamber when applying voltage, and Figure 6 shows examples of the acoustic wave signals detected by the AE measuring system. The average applied and output voltage depending on the volume of particles are shown in Figure 7. As the volume increased, the average applied voltage decreased, and the average output voltage measured by the system increased. The electric field was from 0.5 to 0.9 kV/mm to move the particles. In terms of the particle materials, the magnitude of the acoustic wave signals produced by the aluminum particles was the smallest. Therefore, the aluminum particles, which had the lowest volume, were selected for the actual factory test.

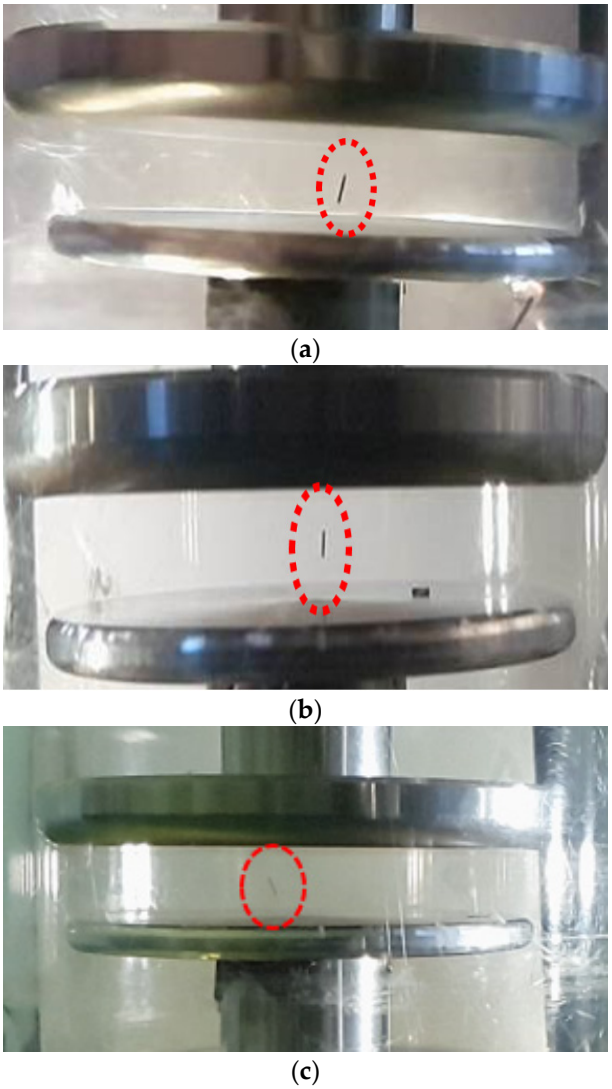

Figure 5. Examples of moving particles in acrylic chamber when applying voltage: (**a**) aluminum, (**b**) copper, (**c**) iron.

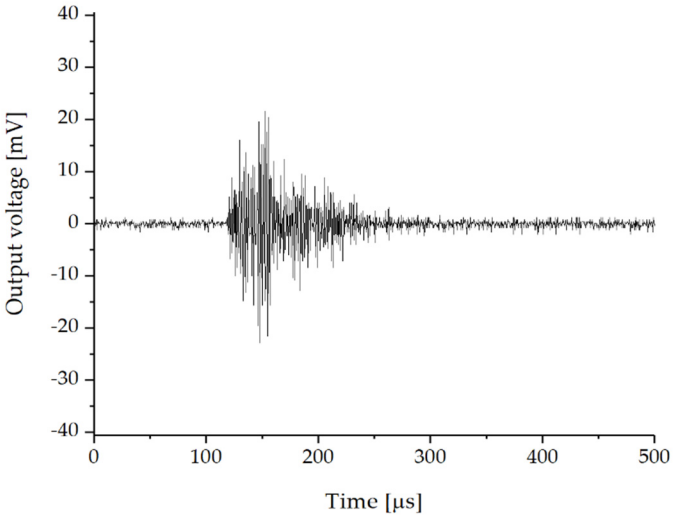

Figure 6. Example of detected acoustic wave signals by AE measuring system.

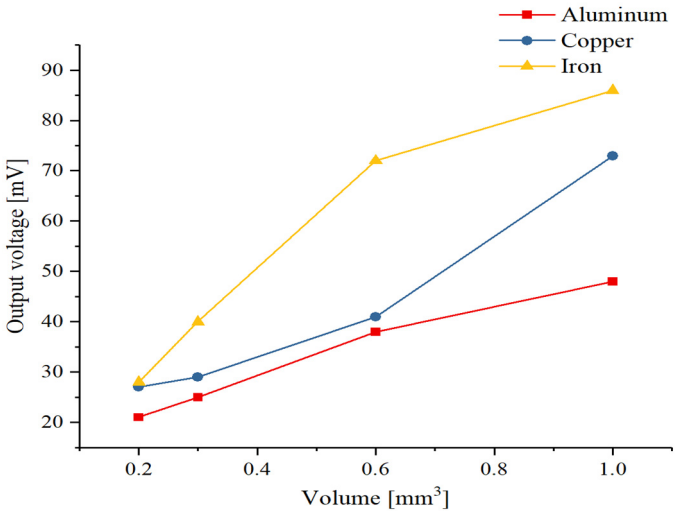

Figure 7. Average applied and output voltage of particle materials depending on volume.

4. Actual Factory Test

4.1. Signal Measurement

To simulate the actual GIS conditions, a mock-up GIS chamber was fabricated, as shown in Figure 8. The chamber was designed to change the distance between the conductor and the enclosure to 20, 27, 32, and 37 mm, and to allow the movement of particles to be visually checked through the inspection window. As the voltage was increased in 1 kV increments to the bushing, the acoustic wave signals produced by the movement of the aluminum particles were detected by the AE measuring system. Figure 9 shows the average applied and output voltage when the particles were moving by the AE measuring system. The longer the distance, the higher the applied voltage when the particle was moving. For this reason, the electric field was 0.7 to 1.0 kV/mm—which was almost constant—to move the particles regardless of the distance. The average output voltage was from 224 to 301 mV depending on the electric field.

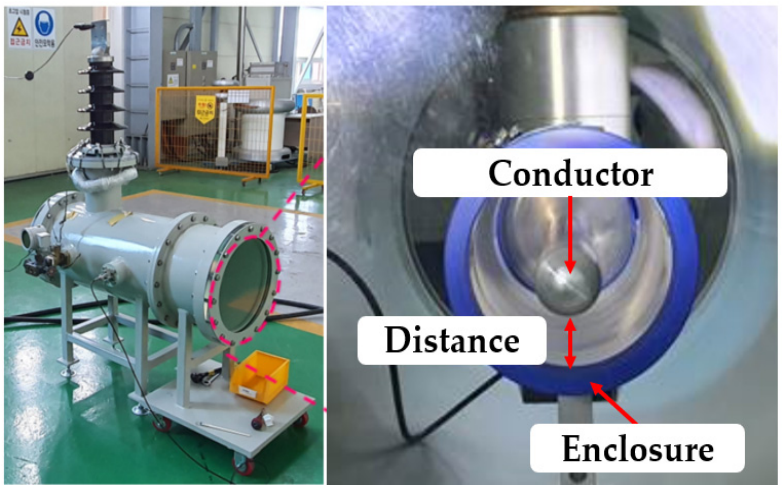

Figure 8. Experimental setup for signal measurement in an actual factory test.

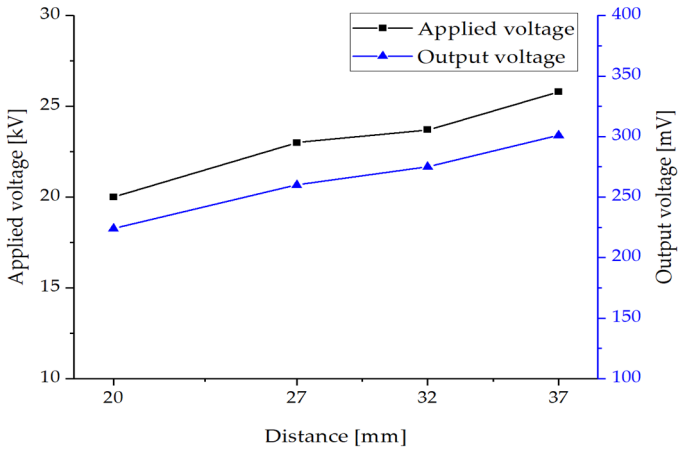

Figure 9. Average applied and output voltage of particle materials depending on distance.

4.2. Signal Attenuation

An acoustic wave signal is attenuated depending on its propagation path and the distance between the sensor and the signal inside a GIS. In [27], the signal attenuation was theoretically 6 dB at 300 mm from the source in a GIS without a flange. Based on the result, three AE sensors were placed under more severe conditions, as shown in Figure 10. To detect the acoustic wave signals produced by a moving aluminum particle with a diameter of 0.25 mm and length of 3 mm, sensor A was installed near the source and sensor B was attached on the bottom of the enclosure 500 mm from the source without a flange. Sensor C was placed on the bottom of the enclosure 500 mm from the source with a flange.

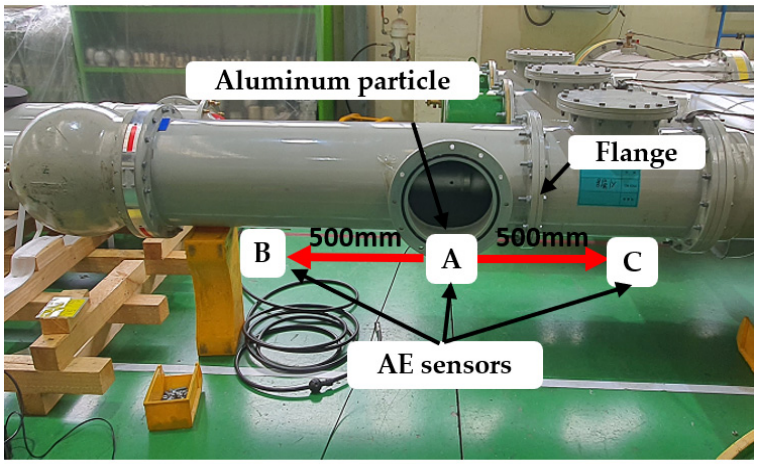

Figure 10. Experimental setup for signal attenuation in an actual factory test.

The applied voltage was increased until the particle moved, and the acoustic wave signal was detected by the three AE sensors at the same time. Figure 11 shows the output voltages measured by each sensor. When the output voltage detected by sensor A was 287 mV, the output voltage detected by sensor B was 127 mV, which was attenuated by 56%. The output voltage of sensor C was 54 mV, which was attenuated by 81% due to the flange. From the result, it was confirmed that the detectable minimum output voltage of the AE measuring system proposed in this paper would be 112 mV for an aluminum particle with a diameter of 0.25 mm and a length of 3 mm. The maximum distance between the sensors would be within 500 mm without any flanges when the AE sensors are placed on the GIS to detect the acoustic wave signals produced by a moving particle due to the signal attenuation.

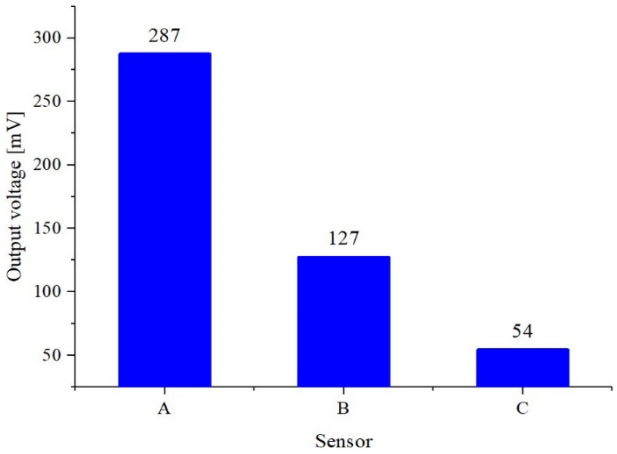

Figure 11. Output voltage of each sensor.

4.3. Study Case

The AE measuring system proposed in this paper was applied to a voltage withstanding test in a 245 kV GIS, as shown in Figure 12a. When a voltage of 110 kV was applied, an acoustic wave signal of 82 mV was measured by the system. Based on the result, a visual inspection was performed, and some particles were found in the circuit breaker with a distance of 92 mm between the conductor and enclosure. The particles were analyzed by energy-dispersive X-ray spectrometry (EDS), as shown in Figure 12b. The particles had metallic and non-metallic components, and the metallic components were composed of iron, zinc, and aluminum. The length of the longest particle was 2.3 mm. Thus, it was estimated that the measured output voltage of the acoustic wave signals produced by the particles with a maximum length of 2.3 mm was lower than the detectable minimum output voltage of the acoustic wave signals produced by the aluminum particles with a length of 3 mm. Figure 13 shows a flowchart of the AE measuring method for the moving particle proposed in this study.

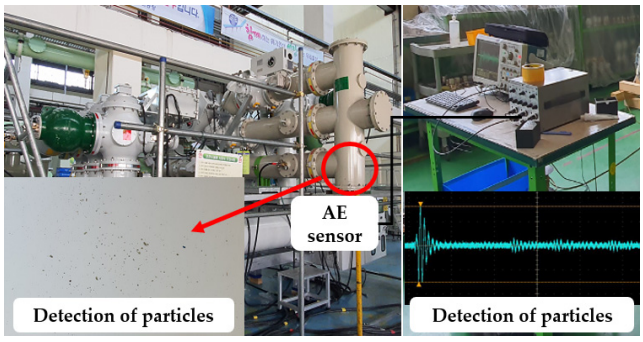

(**a**)

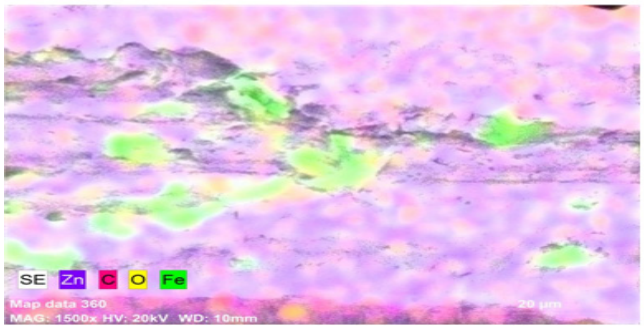

(**b**)

Figure 12. Example of moving particle detection: (**a**) voltage withstanding test, (**b**) EDS result.

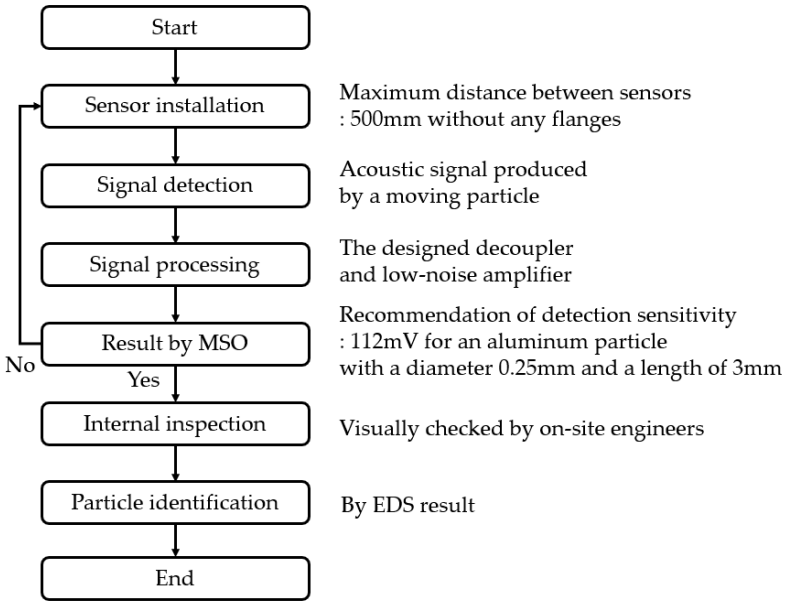

Figure 13. A flowchart of AE measuring method for moving particle detection.

5. Conclusions

An experimental method of detecting moving particles using AE in a GIS was verified in this paper. Twelve types of moving particles with different materials, diameters, and lengths were used, and an AE measuring system, including an AE sensor, a decoupler, and a low-noise amplifier, was designed and fabricated to detect acoustic wave signals with high sensitivity. The results were as follows:

A. In the acrylic chamber, the output voltage was measured to confirm the magnitude of the acoustic wave signals produced by the particles depending on the material and volume and calculated by the diameter and length. The average output voltage of the acoustic wave signals produced by an aluminum particle with a volume of 0.2 mm^3 was the lowest, and it was selected for the actual factory test. The electric field to move the particles was 0.5 to 0.9 kV/mm.

B. In the mock-up GIS, the longer the distance between the conductor and the enclosure, the higher the applied voltage to move the particle. For this reason, the electric field was constant at 0.7 to 1.0 kV/mm to move the particles regardless of the distance. The average output voltage was from 224 to 301 mV depending on the electric field. The signal attenuation of 500 mm in the GIS was 56% without a flange and 81% with a flange. Therefore, the detectable minimum output voltage of the AE measuring system proposed in this paper would be 112 mV and the sensor would be installed at a maximum of 500 mm between sensors without a flange, considering the signal attenuation, to detect moving particles with high sensitivity.

C. In the voltage withstanding test of 245 kV in the GIS, an acoustic wave signal of 82 mV was detected by the AE measuring system proposed in this paper when 110 kV was applied. The electric field to move the particles was 1.2 kV/mm. Some particles were found in the circuit breaker by visual inspection and EDS was performed. Based on the EDS result, some particles were composed of metallic—such as iron, zinc, and aluminum—and non-metallic components. The length of the longest particle was 2.3 mm. For this reason, the measured output voltage of the acoustic wave signals produced by the particles with a maximum length of 2.3 mm was lower than the average output voltage of the acoustic wave signals produced by an aluminum particle with a length of 3 mm.

D. The electric field of the actual GIS was higher than that of the mock-up GIS and acrylic chamber to move the particles in the experimental conditions. It is assumed that the conditions in which the electric field is concentrated are different, such as

the particle types, conductor shapes, GIS structure, and GIS operating status. More studies on the conditions of the electric field to move particles in GISs are needed.

From the results of the experimental validation, the AE measuring system proposed in this paper could detect moving particles clearly in the GIS.

Author Contributions: S.-W.K., N.-H.K. and D.-E.K. conceived and designed the experiments; T.-H.K., Y.-H.C. and D.-H.J. performed the experiments; S.-W.K. and D.-E.K. analyzed the data; G.-S.K. was the supervisor of this work and provided insight and technical expertise to improve the quality of this paper; S.-W.K. and N.-H.K. wrote the paper. All authors have read and agreed to the published version of the manuscript.

Funding: This work was supported by the Technology Innovation Program (No. 20010965, Development of Electronic Current Voltage Transformer and Spacer Based on Eco-Friendly Solid Insulation), funded by the Ministry of Trade, Industry, and Energy (MOTIE), and the Korea Evaluation Institute of Industrial Technology (KEIT) of the Republic of Korea.

Institutional Review Board Statement: Not applicable.

Informed Consent Statement: Not applicable.

Data Availability Statement: Not applicable.

Conflicts of Interest: The authors declare no conflict of interest.

References

1. CIGRE Working Group A3.06. *Final Report of the 2004–2007 International Enquiry on Reliability of High Voltage Equipment*; Technical Brochure No. 513; CIGRE: Paris, France, 2012.
2. International Electrotechnical Commission. *IEC 60071-2: Insulation Coordination-Part 2: Application Guide*; International Electrotechnical Commission: Geneva, Switzerland, 2018.
3. CIGRE Working Group D1.03. *Risk Assessment on Defects in GIS Based on PD Diagnostics*; Technical Brochure No. 525; CIGRE: Paris, France, 2013.
4. CIGRE Joint Working Group 33/23.12. Insulation co-ordination of GIS: Return of experience, on site tests and diagnostic techniques. *Electra* **1998**, *176*, 67–97.
5. International Electrotechnical Commission. *IEC 60270: High-Voltage Test Techniques-Partial Discharge Measurements*; International Electrotechnical Commission: Geneva, Switzerland, 2015.
6. CIGRE Working Group D1.33. *Guide for Partial Discharge Measurements in Compliance to IEC 60270*; Technical Brochure No. 366; CIGRE: Paris, France, 2008.
7. Kim, S.-W.; Jung, J.-R.; Kim, Y.-M.; Kil, G.-S.; Wang, G. New diagnosis method of unknown phase-shifted PD signals for gas insulated switchgears. *IEEE Trans. Dielectr. Electr. Insul.* **2018**, *25*, 102–109. [CrossRef]
8. Ilkhechi, H.D.; Samimi, M.H. Applications of the acoustic method in partial discharge measurement: A review. *IEEE Trans. Dielectr. Electr. Insul.* **2021**, *28*, 42–51. [CrossRef]
9. Beroual, A.; Haddad, A. Recent advances in the quest for a new insulation gas with a low impact on the environment to replace sulfur hexafluoride (SF6) gas in high-voltage power network applications. *Energies* **2017**, *10*, 1216. [CrossRef]
10. Wu, M.; Cao, H.; Cao, J.; Nguyen, H.-L.; Gomes, J.B.; Krishnaswamy, S.P. An overview of state-of-the-art partial discharge analysis techniques for condition monitoring. *IEEE Trans. Power Deliv.* **2015**, *31*, 22–35. [CrossRef]
11. Pearson, J.; Farish, O.; Hampton, B.; Judd, M.; Templeton, D.; Pryor, B.; Welch, I. Partial discharge diagnostics for gas insulated substations. *IEEE Trans. Dielectr. Electr. Insul.* **1995**, *2*, 893–905. [CrossRef]
12. International Electrotechnical Commission. *IEC 62478: High Voltage Test Techniques—Measurement of Partial Discharges by Electromagnetic and Acoustic Methods*; International Electrotechnical Commission: Geneva, Switzerland, 2016.
13. Lundgaard, L.E. Particles in GIS: Behaviour and possibilities for characterisation from acoustic signatures. *IEEE Trans. Dielectr. Electr. Insul.* **2001**, *8*, 1064–1074. [CrossRef]
14. Girodet, A.; Meijer, S.; Smit, J. *Development of a Partial Discharge Analysis Method to Assess the Dielectric Quality of GIS*; Report 15-106; CIGRE: Paris, France, 2002.
15. CIGRE Working Group D1.37. *Guidelines for Partial Discharge Detection Using Conventional (IEC 60270) and Unconventional Methods*; Technical Brochure No. 662; CIGRE: Paris, France, 2016.
16. CIGRE Working Group 15.37. *Diagnostic Methods for GIS Insulating Systems*; Report 15/23-01; CIGRE: Paris, France, 1992.
17. CIGRE Working Group D1.33. *High-Voltage On-Site Testing with Partial Discharge Measurement*; Technical Brochure No. 502; CIGRE: Paris, France, 2012.
18. CIGRE Working Group D1.33. *Guidelines for Unconventional Partial Discharge Measurements*; Technical Brochure No. 444; CIGRE: Paris France, 2010.

19. Bargigia, A.; Koltunowicz, W.; Pigini, A. Detection of partial discharges in gas insulated substations. *IEEE Trans. Power Deliv.* **1992**, *7*, 1239–1249. [CrossRef]
20. CIGRE Working Group B3.24. *Benefits of PD Diagnosis on GIS Condition Assessment*; Technical Brochure No. 674; CIGRE: Paris, France, 2017.
21. Gorman, M.R.; Prosser, W.H. AE source orientation by plate wave analysis. *J. Acoust. Emiss.* **1990**, *9*, 283–288.
22. Lundgaard, L.E. Partial discharge—Part VIII: Acoustic partial discharge detection—Fundamental considerations. *IEEE Electr. Insul. Mag.* **1992**, *8*, 25–31. [CrossRef]
23. Li, X.; Li, J. Acoustic method for multiple free metallic particle recognition in GIS/GIL. *IEEE Trans. Power Deliv.* **2021**, 1. [CrossRef]
24. Sikorski, W. Development of acoustic emission sensor optimized for partial discharge monitoring in power transformers. *Sensors* **2019**, *19*, 1865. [CrossRef] [PubMed]
25. Kil, G.S.; Park, D.W.; Kim, I.K.; Choi, S.Y. Analysis of partial discharge in insulation oil using acoustic signal detection method. *WSEAS Trans. Pow. Syst.* **2008**, *3*, 90–94.
26. Kil, G.-S.; Kim, I.K.; Park, D.-W.; Choi, S.-Y.; Park, C.-Y. Measurements and analysis of the acoustic signals produced by partial discharges in insulation oil. *Curr. Appl. Phys.* **2009**, *9*, 296–300. [CrossRef]
27. Lundgaard, L.; Runde, M.; Skyberg, B. Acoustic diagnosis of gas insulated substations: A theoretical and experimental basis. *IEEE Trans. Power Deliv.* **1990**, *5*, 1751–1759. [CrossRef]